

## Collective intersubband resonances of inversion electrons on GaAs

E. Batke

*Institut für Angewandte Physik, Universität Hamburg, Jungiusstrasse 11, D-2000 Hamburg 36, Federal Republic of Germany*

G. Weimann

*Walter-Schottky-Institut, Technische Universität München, D-8046 Garching, Garching bei München, Federal Republic of Germany*

W. Schlapp

*Forschungsinstitut der Deutschen Bundespost, Postfach 5000, D-6100 Darmstadt, Federal Republic of Germany*

(Received 9 January 1989)

Collective intersubband resonance of inversion electrons in gated AlAs-GaAs single heterojunctions is studied with Fourier-transform spectroscopy using grating coupler techniques. Large grating periods are chosen to test the interface potential at nearly zero wave-vector transfer  $q$  parallel to the sample plane. With highly efficient grating couplers up to three intersubband transitions are excited simultaneously. A coupling of the collective intersubband resonance to confined AlAs optical phonons is observed.

Intersubband resonance (ISR) experiments provide a sensitive test of the interface potential of quasi-two-dimensional (2D) space-charge layers. The subband ladder of electron space-charge layers on GaAs was probed with far-infrared<sup>1-4</sup> (FIR) and Raman<sup>5</sup> spectroscopy by various authors. Because of the symmetry of the GaAs conduction band, ISR can only directly be excited with a FIR electric field component polarized perpendicularly to the interface. This demands special experimental arrangements such as tilted magnetic field configurations<sup>1-3</sup> or FIR reflection at glancing incidence.<sup>4</sup> So far, FIR experiments have been restricted to ISR transitions from the ground to the first excited subband and were obtained mainly via studies of intersubband Landau-level coupling. Here we report directly excited collective ISR transition energies of electron inversion layers on GaAs from the ground to higher subbands covering a wide range of charge densities  $N_s$ ,  $0 \lesssim N_s \lesssim 2.5 \times 10^{11} \text{ cm}^{-2}$ . Three ISR transitions are detected which provide a sensitive test of the interface potential. In addition, we observe coupling of the collective ISR to confined optical phonons of the layers adjacent to the inversion channel, demonstrating the importance of electron-phonon interaction for our experiment.

Gated modulation doped AlAs-GaAs heterojunctions are investigated with Fourier-transform spectroscopy ( $80\text{--}500 \text{ cm}^{-1}$ ). In our transmission geometry with perpendicularly incident FIR radiation the electric field component to excite intersubband transitions is provided by a grating coupler<sup>6,7</sup> prepared on top of the sample. The grating coupler induced electric field at the position of the inversion channel can be expressed in the form  $E = (E_{ox} + E_{qx}, 0, E_{qz})$ , where the  $x$  direction lies in the sample plane perpendicular to the grating stripes and the  $z$  direction parallel to the sample normal.  $E_{ox}$  represents an ordinary transverse wave, whereas  $E_{qx}$  and  $E_{qz}$  represent longitudinal and transverse waves, respectively, that induce a wave-vector transfer  $q_n = 2\pi n/a$  ( $n = 1, 2, \dots$ )

parallel to the interface.  $E_{qx}$  can excite 2D plasmons<sup>8</sup> and  $E_{qz}$  collective intersubband resonances.<sup>6,7</sup> It is well known that ISR experiments excited with a transverse field  $E_{oz}$  at  $q=0$  deviate in energy from the subband separations due to the depolarization shift and the excitonlike correction.<sup>9</sup> Collective ISR experiments excited at finite  $q$  represent nonvertical transitions that are shifted in addition via a collective contribution arising from coupling to 2D plasmons and  $q$ -dependent corrections to the depolarization shift and the final-state interaction.<sup>9-12</sup> Our grating coupler period  $a = 2 \mu\text{m}$  is sufficiently large such that this correction is small and we obtain intersubband optical transition energies at almost a zero wave-vector transfer. In order to suppress the influence of higher-order Fourier components  $q_n$  ( $n \geq 2$ ) the grating strip width compared to the period  $a$  is designed to be 0.5.

Our heterojunctions are grown by molecular-beam epitaxy on semi-insulating GaAs substrates and are of special design. On top of a buffer layer of about  $1\text{-}\mu\text{m}$  GaAs the usual  $\text{Al}_x\text{Ga}_{1-x}\text{As}$  alloy is replaced by a short-period AlAs-GaAs superlattice of twenty periods. The individual AlAs and GaAs layer thicknesses are 2 and 1.5 nm, respectively. The eighth GaAs layer from the top is  $\delta$  doped with Si to a concentration of  $1.25 \times 10^{13} \text{ cm}^{-2}$ . A 9-nm cap layer of doped GaAs completes the sequence. A thin continuous metal layer of NiCr with sheet resistance  $R_g = 1000 \Omega/\square$  serves as a gate to vary  $N_s$  via the field effect. Four contacts are provided to determine  $N_s$  via Shubnikov-de Haas or, alternatively, via magnetocapacitance measurements. The sample has a density of  $(2.0 \pm 0.1) \times 10^{11} \text{ cm}^{-2}$  at zero gate voltage and a mobility in excess of  $5 \times 10^5 \text{ cm}^2/\text{Vs}$  at 2 K.  $N_s$  changes almost linearly with  $V_g$  and the conductivity threshold is at  $V_g = -340 \text{ meV}$ .

Figure 1 shows collective ISR measured at 2 K. We plot the relative change in transmission  $-\Delta T/T = [T(0) - T(N_s)]/T(0)$  with  $T(0) = T(V_g = -1 \text{ V})$  for different  $N_s$ . Since we are in the electric quantum limit only inter-

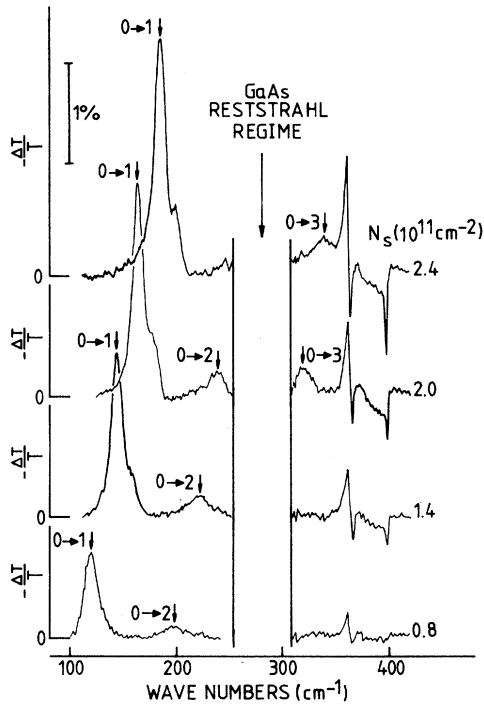


FIG. 1. Relative change in transmission  $-\Delta T/T$  of  $n$ -type AlAs-GaAs single heterojunctions vs frequency for different  $N_s$ . Resonance positions are marked by arrows and labeled  $0 \rightarrow n$  ( $n=1,2,3$ ). The GaAs reststrahl regime (260–310  $\text{cm}^{-1}$ ) is not accessible in transmission.

subband transitions from the ground ( $n=0$ ) to higher subbands ( $n \geq 1$ ) are possible. ISR positions are marked by arrows and labeled  $0 \rightarrow n$ . At  $N_s = 2 \times 10^{11} \text{ cm}^{-2}$  three transitions are observed simultaneously. In the reststrahl regime of GaAs ranging from about 260 to 310  $\text{cm}^{-1}$  the radiation is blocked. With decreasing  $N_s$  all ISR positions shift to lower frequencies. The  $0 \rightarrow 3$  transition merges into, whereas the  $0 \rightarrow 2$  transition emerges from, the GaAs reststrahl regime with reduced  $N_s$ .

The line shape of the  $0 \rightarrow 1$  ISR transition exhibits a satellite peak at its high-energy side. Magnetocapacitance measurements give two discrete densities  $N_{s1} = 2 \times 10^{11} \text{ cm}^{-2}$  and  $N_{s2} = 2.2 \times 10^{11} \text{ cm}^{-2}$  at  $V_g = 0$ . Surface acoustic wave attenuation measurements performed on samples from the same wafer indicate that about 10% of the active sample area has a higher density.<sup>13</sup> Thus, the observed line shape is a superposition of two ISR at slightly different  $N_s$ . Because of the limited signal-to-noise ratio satellite peaks are not resolved for the transitions  $0 \rightarrow 2$  and  $0 \rightarrow 3$ .

The full width at half maxima of the ISR are  $\Delta\omega_{01} = 14 \text{ cm}^{-1}$  and  $\Delta\omega_{02} \approx \Delta\omega_{03} \approx 20 \text{ cm}^{-1}$  independent of  $N_s$ . Usually the ISR half-width is expected to depend on the individual intraband scattering times of the subbands participating in the excitation process and a contribution from intersubband scattering.<sup>14</sup> Numerical values for our GaAs heterojunction are not available from which we could calculate the ISR half-width. Half-widths estimated from the mobility are less than  $0.6 \text{ cm}^{-1}$ , much smaller

than observed. Cyclotron resonance and plasmon resonance half-widths measured at small magnetic fields  $B \approx 1 \text{ T}$  on the same sample are also more than 1 order of magnitude smaller, e.g., at  $N_s = 2 \times 10^{11} \text{ cm}^{-2}$  the cyclotron resonance and plasmon resonance half-widths are 0.8 and 1.0  $\text{cm}^{-1}$ , respectively. The plasmon resonance half-width is larger than the cyclotron resonance half-width and indicates the presence of inhomogeneous broadening.<sup>15</sup> Thus, we also expect a contribution of inhomogeneous broadening to the large ISR half-width.

In Fig. 2 all ISR positions are summarized. The resonance positions show nearly a linear dependence on  $N_s$  and extrapolate to finite energies at  $N_s = 0$ . The latter is expected in the presence of a finite depletion charge, i.e., for inversion conditions. The solid line are calculated subband separations  $E_{10}$  for three different depletion charges  $N_{\text{depl}}$  taken from Ref. 16. The  $0 \rightarrow 1$  resonance energy extrapolates at  $N_s \rightarrow 0$  to 94  $\text{cm}^{-1}$  close to the extrapolated subband separation  $E_{10}$  for  $N_{\text{depl}} = 0.46 \times 10^{11} \text{ cm}^{-2}$ . The extrapolated  $N_s \rightarrow 0$  limits of the transitions  $0 \rightarrow 2$  and  $0 \rightarrow 3$  are 174 and 217  $\text{cm}^{-1}$ , respectively. Assuming  $N_{\text{depl}} = 0.5 \times 10^{11} \text{ cm}^{-2}$  this fits well to subband separations  $E_{10} = 92 \text{ cm}^{-1}$ ,  $E_{20} = 167 \text{ cm}^{-1}$ , and  $E_{30} = 233 \text{ cm}^{-1}$  calculated in triangular-well approximation. With increasing  $N_s$  the  $0 \rightarrow 1$  ISR transition energy exhibits a steeper slope than the calculated subband separation  $E_{10}$ . This is thought to arise from the  $N_s$  dependence of the depolarization shift and the final-state interaction which raise the ISR transition energies compared to the subband separations.

In Fig. 3 we show sharp spectral structures that are apparent in Fig. 1 at high wave numbers  $\nu > 310 \text{ cm}^{-1}$  on an expanded energy scale. There is a derivative-type

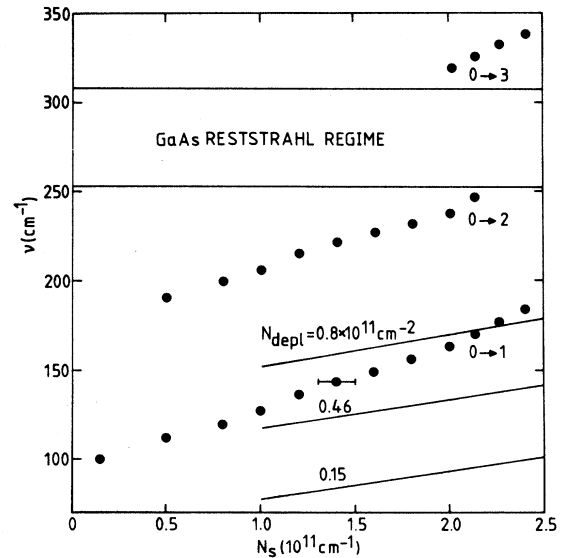


FIG. 2. Intersubband optical transition energies of inversion electrons on GaAs vs  $N_s$ . Three transitions  $0 \rightarrow n$  from the ground subband are indicated. The solid lines are theoretical subband separations  $E_{10}$  from Ref. 16 for three different depletion charges  $N_{\text{depl}}$ . The horizontal lines mark the reststrahl regime of GaAs.

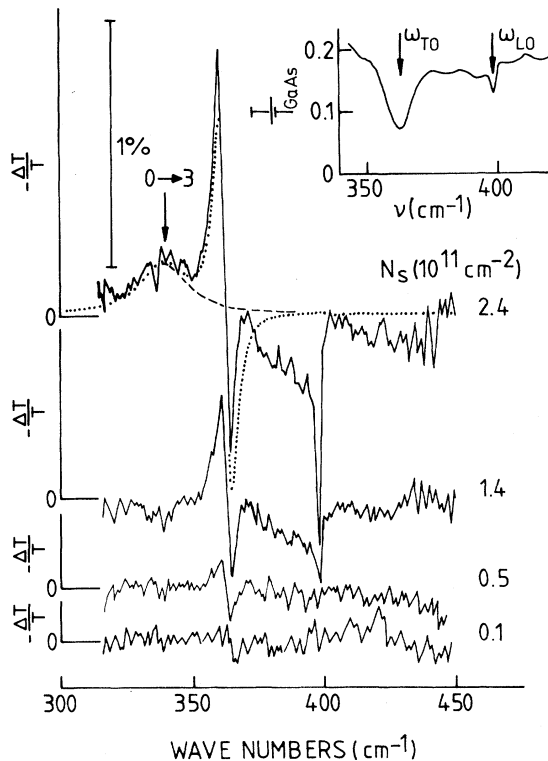


FIG. 3. Expanded view at  $-\Delta T/T$  in the vicinity of the optical-phonon frequencies of AIAs for different  $N_s$ . The inset compares the sample transmission  $T$  to the transmission  $T_{\text{GaAs}}$  of a GaAs substrate. The  $0 \rightarrow 3$  ISR transition energy is marked by an arrow. Dashed and dotted lines are calculated as described in the text.

modulation around  $363 \text{ cm}^{-1}$  and a sharp dip at about  $398 \text{ cm}^{-1}$ . Both structures decrease linearly in strength with  $N_s$  and disappear at the conductivity threshold. Their positions, to be discussed in more detail below, are close to the confined AIAs-like optical-phonon frequencies of a short-period GaAs-AIAs superlattice.<sup>17-19</sup> The appearance of phonon structures in  $-\Delta T/T$  arises naturally from the electron-phonon interaction in our samples. In earlier FIR spectroscopical studies of Si metal-oxide-semiconductor systems Fano-type ISR line-shape anomalies were observed for hole space-charge layers at the optical-phonon frequency of Si.<sup>20</sup> For electron space-charge layers a coupling of the ISR to the longitudinal optical phonon of the adjacent  $\text{SiO}_2$  layer was reported.<sup>7</sup> The phonons to be discussed here are confined AIAs optical phonons associated with the GaAs-AIAs superlattice adjacent to the space-charge layer.

The inset of Fig. 3 shows the transmission of our samples normalized to the transmission of a GaAs substrate, reflecting the AIAs-GaAs superlattice phonon absorption. Two absorption lines labeled  $\omega_{\text{TO}}$  and  $\omega_{\text{LO}}$  are marked in position. In our transmission geometry with normally incident FIR radiation the grating coupler allows coupling to various phonons. The field component  $E_{ox}$  can couple to the transverse optical phonon at  $q=0$ , whereas the spa-

tially modulated field  $(E_{qx}, 0, E_{qz})$  can couple to longitudinal optical (LO), transverse optical (TO), and interface phonons at defined wave vector  $q$ . The frequencies  $\omega_{\text{TO}} = (363 \pm 0.5) \text{ cm}^{-1}$  and  $\omega_{\text{LO}} = (399 \pm 0.5) \text{ cm}^{-1}$  represent confined AIAs TO and LO phonons, respectively.<sup>17-19</sup> The absorption line at  $\omega_{\text{TO}}$  is particularly strong and broad  $\Delta\omega_{\text{TO}} \approx 8.5 \text{ cm}^{-1}$ , whereas the line at  $\omega_{\text{LO}}$  is weaker but considerably smaller  $\Delta\omega_{\text{LO}} \approx 2.5 \text{ cm}^{-1}$ .

We explain the spectral structures in  $-\Delta T/T$  at the AIAs LO phonon energy as caused by the  $N_s$  dependence of collective intersubband plasmon-phonon modes.<sup>21-23</sup> At finite  $q$  all individual modes are coupled, and via  $N_s$  changes in resonance positions will be reflected in  $-\Delta T/T$ . Since the LO phonons are localized in the AIAs layers a coupling to the inversion electrons requires a penetration of the electron wave function into the adjacent AIAs slabs. With increasing  $N_s$  the electrons are pushed closer to the interface and will interact more strongly with the LO phonon as observed experimentally. The phonon structures associated with the AIAs TO phonon is striking. It is well known that inversion electrons at the interface of two semi-infinite polar dielectrics can couple to LO but not to TO bulk phonons.<sup>22</sup> In Fig. 3 at  $N_s = 2.4 \times 10^{11} \text{ cm}^{-1}$  the  $0 \rightarrow 3$  ISR transition is close to the AIAs TO phonon, and one might argue that the phonon structure is of purely dielectric origin, arising from mixed electronic and phonon contributions to the transmission. Using classical frequency-dependent dielectric functions, we have calculated  $-\Delta T/T$  for our samples assuming  $p$ -polarized incident FIR radiation, a fixed AIAs TO frequency, and an ISR transition energy close to  $\omega_{\text{TO}}$  as shown in Fig. 3 with a dashed line. We find negligible phonon features in the calculated spectra. If a nearby intersubband transition would induce the phonon feature, one would expect this feature to disappear if there is negligible overlap between electronic and phonon-induced absorption contributions. However, at  $N_s = 1.4 \times 10^{11} \text{ cm}^{-1}$  the  $0 \rightarrow 3$  ISR has vanished already, but the phonon feature still persists.

This phonon feature is consistent with a shift of the AIAs TO phonon frequency to higher energies with increasing  $N_s$ . As shown in Fig. 3 with a dotted line we can qualitatively explain the experimental  $-\Delta T/T$  if we assume a shift of  $0.25 \text{ cm}^{-1}$  at  $N_s = 2.4 \times 10^{11} \text{ cm}^{-2}$ . In our model calculation we use a phonon damping constant which reproduces the measured width of the AIAs TO absorption line. This treatment is approximative since the grating-coupler-induced TO absorption line is a complex superposition of phonons excited at zero and finite  $q$  which have to be described by individual frequencies, damping constants, and frequency shifts. However, a change in phonon frequency is expected within the framework of coupled intersubband plasmon-phonon modes due an enhanced mode repelling with increasing  $N_s$ . The confinement of TO phonons and the penetration of the electron wave function into the adjacent AIAs slabs are held responsible to induce electron-TO-phonon coupling in our samples.

In summary, collective ISR of inversion electrons on GaAs covering a wide range of charge densities are discussed. Three ISR transitions are observed, indicating that there are at least four confined electronic interface

states. The inversion electrons couple strongly to optical phonons in the adjacent GaAs-AlAs short-period superlattice.  $N_s$ -dependent spectral features at the energies of confined AlAs optical phonons are explained within the framework of coupled intersubband plasmon-phonon modes.

We would like to thank J. P. Kotthaus for valuable discussions and the Deutsche Forschungsgemeinschaft for financial support.

- 
- <sup>1</sup>Z. Schlesinger, J. C. M. Hwang, and S. J. Allen, Jr., Phys. Rev. Lett. **50**, 2098 (1983).
- <sup>2</sup>A. D. Wieck, J. C. Maan, U. Merkt, J. P. Kotthaus, K. Ploog, and G. Weimann, Phys. Rev. B **35**, 4145 (1987).
- <sup>3</sup>K. Ensslin, D. Heitmann, and K. Ploog, this issue, Phys. Rev. B **39**, 10879 (1989).
- <sup>4</sup>A. D. Wieck, K. Bollweg, U. Merkt, G. Weimann, and W. Schlapp, Phys. Rev. B **38**, 10158 (1988).
- <sup>5</sup>G. Abstreiter, M. Cardona, and A. Pinczuk, in *Light Scattering in Solids IV*, edited by M. Cardona and G. Güntherodt, Topics in Applied Physics, Vol. 54 (Springer-Verlag, Berlin, 1984), p. 5.
- <sup>6</sup>E. Batke, D. Heitmann, and E. G. Mohr, Physica **117&118B**, 670 (1983).
- <sup>7</sup>D. Heitmann and U. Mackens, Phys. Rev. B **33**, 8269 (1986).
- <sup>8</sup>E. Batke, D. Heitmann, and C. W. Tu, Phys. Rev. B **34**, 6951 (1986).
- <sup>9</sup>T. Ando, A. B. Fowler, and F. Stern, Rev. Mod. Phys. **54**, 437 (1982).
- <sup>10</sup>A. Tselis and J. J. Quinn, Surf. Sci. **113**, 362 (1982).
- <sup>11</sup>S. Das Sarma, Phys. Rev. B **29**, 2334 (1984).
- <sup>12</sup>R. Sooryakumar, A. Pinczuk, A. Gossard, and W. Wiegmann, Phys. Rev. Lett. **31**, 2578 (1984).
- <sup>13</sup>A. Wixforth, M. Wassermeier, J. Scriba, and J. P. Kotthaus (unpublished); and (private communication).
- <sup>14</sup>T. Ando, J. Phys. Soc. Jpn. **44**, 765 (1978).
- <sup>15</sup>M. Tewordt, E. Batke, J. P. Kotthaus, G. Weimann, and W. Schlapp, in *Proceedings of the International Conference on The Application of High Magnetic Fields in Semiconductor Physics, Würzburg, 1988*, edited by G. Landwehr (Springer-Verlag, Berlin, in press).
- <sup>16</sup>F. Stern and S. Das Sarma, Phys. Rev. B **30**, 840 (1984).
- <sup>17</sup>K. Kubota, M. Nakayama, H. Katoh, and N. Sano, Solid State Commun. **49**, 157 (1984).
- <sup>18</sup>A. K. Sood, J. Menéndez, M. Cardona, and K. Ploog, Phys. Rev. Lett. **54**, 2111 (1985).
- <sup>19</sup>A. Ishibashi, M. Itabashi, Y. Mori, K. Kaneko, S. Kawado, and N. Watanabe, Phys. Rev. B **33**, 2887 (1986).
- <sup>20</sup>D. Heitmann, E. Batke, and A. D. Wieck, Phys. Rev. B **31**, 6865 (1985).
- <sup>21</sup>J. I. Gersten, Surf. Sci. **97**, 206 (1980).
- <sup>22</sup>L. Wendler, Phys. Status Solidi **129**, 513 (1985).
- <sup>23</sup>L. Wendler and R. Pechstedt, Phys. Status Solidi **141**, 129 (1987).